

Distinguishing Multispin Interactions from Lower-Order Effects

Thomas R. Bergamaschi,^{1,*} Tim Menke^{1,2,3,†}, William P. Banner,⁴
 Agustin Di Paolo², Steven J. Weber,⁵ Cyrus F. Hirjibehedin^{1,5}, Andrew J. Kerman,⁵ and
 William D. Oliver^{1,2,4,5,‡}


¹*Department of Physics, Massachusetts Institute of Technology, Cambridge, Massachusetts 02139, USA*

²*Research Laboratory of Electronics, Massachusetts Institute of Technology, Cambridge, Massachusetts 02139, USA*

³*Department of Physics, Harvard University, Cambridge, Massachusetts 02138, USA*

⁴*Department of Electrical Engineering and Computer Science, Massachusetts Institute of Technology, Cambridge, Massachusetts 02139, USA*

⁵*Lincoln Laboratory, Massachusetts Institute of Technology, Lexington, Massachusetts 02421-6426, USA*

 (Received 10 January 2022; revised 17 August 2022; accepted 18 August 2022; published 7 October 2022)

Multispin interactions can be engineered with artificial quantum spins. However, it is challenging to verify such interactions experimentally. Here, we describe two methods to characterize the n -local coupling of n spins. First, we analyze the variation of the transition energy of the static system as a function of local spin fields. Standard measurement techniques are employed to distinguish n -local interactions between up to five spins from lower-order contributions in the presence of noise and spurious fields and couplings. Second, we show a detection technique that relies on time-dependent driving of the coupling term. Generalizations to larger system sizes are analyzed for both static and dynamic detection methods and we find that the dynamic method is asymptotically optimal when increasing the system size. The proposed methods enable robust exploration of multispin interactions across a broad range of both coupling strengths and qubit modalities.

DOI: [10.1103/PhysRevApplied.18.044018](https://doi.org/10.1103/PhysRevApplied.18.044018)

I. INTRODUCTION

Although interactions that depend on more than two spins are usually not present in natural quantum spin systems, they are a key resource for analog quantum simulation and quantum computation applications. For example, multispin interactions arise in the mapping of fermions to artificial spin systems in quantum algorithms for quantum chemistry [1–3] or in effective spin models of cuprate superconductor Hamiltonians [4]. In addition, multispin interactions play a crucial role in error-suppression schemes for quantum annealers [5,6], in adiabatic topological quantum computation [7], as well as in a variety of combinatorial optimization problems [8–10]. Such multispin interactions are called n -local when there are n spins partaking in a single many-body coupling mechanism.

While many n -local coupling proposals use perturbative Hamiltonian gadgets with ancilla qubits to obtain the effective interaction [11–14], a variety of nongadgetized 3- and 4-local interaction schemes have been proposed

[15–20], some of which are scalable to higher-order locality. While the implementation of such interactions appears to be of broad interest, the identification of multispin interactions when these are relatively weak and appear in combination with interactions of other orders that are of comparable strength or larger remains an open question. In addition, some coupling mechanisms can cause further undesired couplings of lower order [17–19], requiring detection methods that reliably determine the coupling despite such spurious terms.

In this work, we propose error-resilient methods for the characterization of multispin interactions. The studied methods can be split into two classes: one relying on the static properties of an n -local Hamiltonian and the other exploiting time-dynamic effects when driving such a Hamiltonian. For the static detection technique, we rely only on spectroscopic measurements rather than temporal dynamics. Naturally, this method is directly relevant for experiments with artificial spin systems that exhibit limited coherence. Using Hamiltonian model fits, which are commonly employed to characterize artificial spin systems [21–23], we find numerical evidence that the n -local interaction adds a unique signature to the behavior of the transition energy of the system when local spin fields are varied. We study the robustness of this

*thomasbe@mit.edu

†timmenke@mit.edu

‡william.oliver@mit.edu

technique by analyzing the performance of the method in the presence of emulated experimental noise, which dampens the size of the n -local coupling signature. This static method is contrasted with a time-dependent detection technique that requires a stronger set of assumptions on the experimental system control. In this case, the capability of detecting n -local interactions scales more favorably with system size and we find that it is an asymptotically optimal detection technique. However, it is subject to stringent coherence-time requirements. By contrasting detection-method classes with high and low experimental-control requirements, we identify their respective merits for practical quantum device characterization. We note that techniques related to those presented in this paper have been used to demonstrate tunable three-body interactions between superconducting qubits in Ref. [24].

II. COUPLED MULTISPIN HAMILTONIANS

We consider an n -spin system in which all subsets of spins are coupled. Additionally, we consider that the system has a *coupler* as portrayed in Fig. 1. We assume that the coupler can be turned on and off. When it is on, it adds an n -local term to the Hamiltonian that couples all spins and takes the form $MZ_1 \otimes Z_2 \otimes \dots \otimes Z_n$ in the system Hamiltonian. The n -local coupling strength is given by M , and Z_i is the Pauli Z matrix for the i th spin.

The following n -spin Hamiltonian family is considered:

$$H = \sum_{s \in S} \delta_s X_s + \epsilon_s Z_s + \sum_{Q \subseteq S, |Q| > 1} J_Z^{(Q)} \bigotimes_{s \in Q} Z_s + J_X^{(Q)} \bigotimes_{s \in Q} X_s, \quad (1)$$

where X_i and Z_i are the X and Z Pauli matrices, respectively. The first sum is over individual spins in the set S of all n spins and the second runs over all nonempty subsets Q of size larger than one. For each spin subset Q , the Hamiltonian defines a coupling between all spins in the subset, which can be a Z -type coupling with strength $J_Z^{(Q)}$ or an X -type coupling with strength $J_X^{(Q)}$. We only consider Z coupling and transverse X terms but our techniques can be generalized to include Y -type coupling. Inspired by the relevant platform of single-loop flux qubits [25–27], we assume that the single-spin Z fields ϵ_s are the only tunable parameters in this Hamiltonian apart from the ability to turn the coupler on and off. We can vary each ϵ_s parameter for each spin s individually in the range from 0 to ϵ_{\max} . Similarly, we label by δ_s the single-spin X field, which is not tunable. The n -local term of interest is present when $Q = S$. We assume the n -local term along the X direction to be fixed to $J_X^{(S)} = 0$ and we define $J_Z^{(S)} = M$. For the system model, we use parameters that are experimentally feasible for coupled superconducting flux qubits, a promising platform for realizing artificial spin systems. We

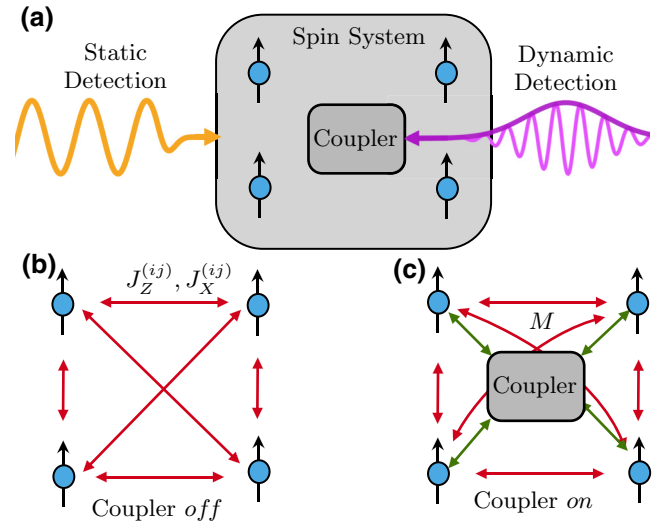


FIG. 1. A system of artificial spins coupled via a multispin coupler. (a) The types of techniques to detect multispin interactions considered in this work. Static detection techniques probe steady-state behavior with continuous-wave drives, whereas dynamic techniques such as coupler pulses lead to transient behavior. (b) A schematic of the system for $n = 4$ when the coupler is off, including pairwise interactions J_Z and J_X between all pairs of spins. (c) When the coupler is turned on, a 4-local term with coupling strength M as well as spurious terms of lower locality are added to the system Hamiltonian.

set $\delta_s = 2\pi \times 2$ GHz, $\epsilon_{\max} = 2\pi \times 10$ GHz for the single-qubit fields and for the coupling parameters of locality lower than n we assume $J_X^{(Q)}$ and $J_Z^{(Q)}$ to be sampled in the range of $2\pi \times [0, 300)$ MHz [21,22]. Finally, for the n -local term, we base our values on the practical coupler proposal discussed in Ref. [19], which estimates a 4-local coupling of about $2\pi \times 500$ MHz. However, we expect that the first experimental prototypes will exhibit a lower coupling and we assume $M = 2\pi \times 50$ MHz. Although these Hamiltonian parameters are aimed at highlighting experimental feasibility, we emphasize that our techniques are also applicable to other systems encoding artificial spins. We note that the conclusions presented in this paper can be applied to other values of M by scaling the Hamiltonian parameters appropriately. In this way, the performance for smaller coupling terms M has been studied by rescaling the other interaction terms; in particular, increasing the magnitude of the spurious terms. In Sec. III of the Supplemental Material [28], we analyze this dependence and show that rescaling the spurious terms does not significantly affect the detection method.

Throughout this work, we denote a k -local coupling term as an additive term in the Hamiltonian of the form $Z_1 \otimes Z_2 \otimes \dots \otimes Z_k$ (or along the X direction) between any group of k spins. Similarly, we define a k -local Hamiltonian as including l -local coupling terms from $l = 1$ to

$l = k$. The *locality* of such a k -local Hamiltonian is the quantity k .

Most practical n -local coupler setups, as in Refs. [17–19], will be imperfect. Whenever the coupler is turned on, it generates spurious terms, inadvertently altering all other Hamiltonian parameters—except the n -local parameters $J_X^{(S)}$ and $J_Z^{(S)}$ —by a value in the range $\pm\eta M$, where η is the relative spurious-term amplitude. Here, we consider η fixed at $\eta = 1/2$ but we generalize to include larger values of η in Sec. I of the Supplemental Material [28].

III. STATIC DETECTION TECHNIQUE

The first proposed detection technique is based on analyzing variations in the transition energy between the ground and first excited state of the system both with the coupler on and off. The detection principle is based on the fact that these variations contain an n -local signature, which can only be generated by a Hamiltonian with the desired n -local term and not with an $(n - 1)$ -local Hamiltonian. The proposed experimental procedure consists of measuring the transition energy first with the coupler off $E_{01}^{(0)}$, then on $E_{01}^{(M)}$, and analyzing the variation of the transition energy:

$$\{\Delta E^M\} = \{E_{01}^{(M)} - E_{01}^{(0)}\}. \quad (2)$$

The transition-energy variation ΔE^M is determined as a function of the tunable Z fields ϵ_i while maintaining some of the spins fixed at $\epsilon_i = 0$. Specifically, for each subset of spins $Q \subseteq S$, we set $\epsilon_i = \epsilon \forall i \in Q$ and measure the transition-energy variation as a function of ϵ , varying from 0 to ϵ_{\max} . Doing so for all subsets of spins, we calculate the transition-energy variation as a function of ϵ for $2^n - 1$ distinct configurations, as visualized in Fig. 2. Many of these curves do not simply collapse onto each other due to the sampled spurious terms, which break the system degeneracy.

In this paper we show that the spectroscopy curves contain an n -local *signature*, which can only be explained by an n -local Hamiltonian and by none other with lower locality. We find the signature via a pair of Hamiltonian model fits based on Eq. (1). Specifically, we assume that we know all original coupling parameters with the coupler off. Experimental techniques exist to characterize such 1- and 2-local terms reliably [21–23,29]. Using a least-squares fitting procedure [30], one fit is then performed with an n -local Hamiltonian and another with an $(n - 1)$ -local Hamiltonian. The fits determine all spurious shifts and the n -local term. By comparing the two fits via a fit-quality measure, we can differentiate whether the system is described by an n -local Hamiltonian or one of lower locality. Fewer than the $2^n - 1$ spin configurations can be used for the curve fits or the ϵ parameters can be chosen differently for different spins. We do not analyze such

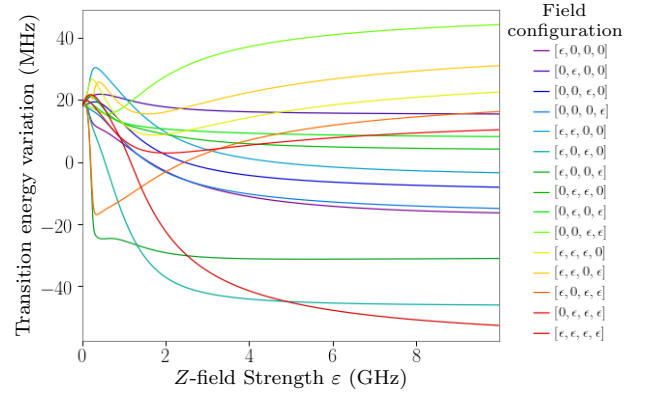


FIG. 2. The transition-energy variation of a 4-spin system. It is shown how the transition-energy variation changes with the local Z field ϵ for all field configurations. The legend indicates to which of the 4-spins the field is applied for each curve.

modifications here but they could potentially result in more scalable and efficient detection methodologies.

To analyze the performance of the fits on the n -local Hamiltonian data, we introduce a quality measure. The first measure is the mean deviation between the fitted curve and the data points corresponding to the n -local Hamiltonian data. Under the assumption of no experimental error, this quality measure easily distinguishes between an n -local and an $(n - 1)$ -local Hamiltonian model, concluding that the system Hamiltonian indeed includes an n -local term. To study the procedural robustness, we analyze whether we can still distinguish the two Hamiltonian models in the presence of noise.

IV. SPECTRAL RESOLUTION THRESHOLD

We analyze the robustness of the proposed detection method against emulated experimental errors. Specifically, we introduce noise to the generated data and analyze how both the n -local and $(n - 1)$ -local Hamiltonian models perform. As we increase the noise amplitude σ , we expect the quality of the n -local model to worsen, until the quality of both models is comparable. In this limit, we can no longer characterize whether or not the system exhibits n -local coupling.

To emulate noise with amplitude σ , we randomly shift each transition-energy data point by an error $\xi \sim \mathcal{N}(0, \sigma^2)$ drawn from a normal distribution with mean 0 and variance σ^2 . In this way, we emulate the spectral line width of a spin transition with coherence time $T_2 = 1/(2\pi\sigma)$, which creates an uncertainty in the transition-frequency measurement. We then analyze the quality measure of both the n -local and $(n - 1)$ -local model as we increase σ . We identify a critical noise amplitude σ_C at which the quality of both models is comparable and we can no longer distinguish the Hamiltonian locality.

Figures 3(a) and 3(b) show the transition-energy variation versus flux for a 4-spin system and two different error amplitudes. The fit is performed simultaneously on all 15 field configurations but only one configuration is shown for clarity. As expected, the 4-local model mean deviation is small for small σ , while the 3-local model mean deviation is relatively large, clearly distinguishing the two models. When we increase σ , however, both Hamiltonian fits have large deviations and we cannot distinguish which model better describes the data.

We analyze this behavior more precisely as a function of σ in Fig. 3(c): we increase σ and again compare the mean fit deviation between the two models. The critical noise amplitude σ_C is defined by the intersection point of a pair of linear fits in Fig. 3(c), in which the blue line fits to the 4-local model data, and the orange line to the first five points of the 3-local model data. We highlight that at the intersection point σ_C , we can no longer distinguish between the models. For four spins, the intersection occurs at around $\sigma_C(n=4) = 15$ MHz, which corresponds to $T_2 = 11$ ns. This time is substantially lower than that of state-of-the-art superconducting qubit devices, which have coherence times in the microsecond regime [21,31].

The extension of the error analysis for other system sizes is shown in the inset of Fig. 3(c) and we analyze how the critical noise amplitude varies as a function of the number of spins n . We find that $\sigma_C(n)$ decreases exponentially as a function of n , suggesting the need for exponentially more precise experiments and measurements with increasing system size. See Sec. I of the Supplemental Material [28] for a similar analysis regarding the effect of spurious terms on this detection technique.

V. EXTENSION TO LARGER SYSTEM SIZES

We now approach the detection problem from a more analytical perspective, examining how our proposed method generalizes asymptotically for large n . To derive an asymptotic bound for $\sigma_C(n)$, we make the simplifying assumption that the system has no coupling terms beside the n -local term. We assume that all δ_i parameters are identical to δ and that the n -local term M is small compared to other permanent terms in the Hamiltonian. Moreover, we consider a slightly different measure of fit quality: the mean deviation between the fit and the error-shifted data point, which allows easier theoretical treatment.

We show that $\sigma_C(n)$ varies asymptotically as $O(M/2^n)$. We first give a brief argument for a lower bound of the quality measure of an n -local Hamiltonian fit as a function of σ . Then, we motivate an upper bound for the quality measure of an $(n-1)$ -local Hamiltonian fit. See Sec. II of the Supplemental Material [28] for a proof of these bounds, which require the use of perturbation-theory arguments.

The main result is an exponentially decreasing bound for σ_C of the form

$$\sigma_C = O\left(\frac{M}{2^n} \langle \cos \theta \rangle^n\right), \quad (3)$$

where θ is the angle between the ground state and the Z direction if the system were noninteracting. The exponentially decreasing bound shows us the limitations of the detection method. Our proof is straightforward to generalize to any spectroscopic detection method, as such a technique suffers from an exponentially decreasing error setback. This is true while the system contains small coupling and permanent single-spin X terms, as this guarantees that $\langle \cos \theta \rangle < 1$. Our finding motivates the search for a more generalizable detection technique that can be compared to the spectroscopic method both for required control capabilities and asymptotic scaling.

VI. DYNAMIC DETECTION TECHNIQUE

In addition to the exponential bound for spectroscopic detection schemes, no experimental detection technique is expected to detect n -local coupling while maintaining spectroscopic errors greater than $O(M)$. This implies that to detect an n -local coupling, we require our system to have a coherence time of at least $O(1/M)$. We discuss a dynamic detection technique that achieves this asymptotically optimal bound without suffering from an exponentially decreasing error bound for larger n . The approach is based on exploiting transitions that are prohibited without the presence of an n -local term. Specifically, consider setting all ϵ_i parameters to zero, such that the permanent δ_i parameters are dominant and the system eigenstates are approximate X eigenstates. The ground state is then $|\alpha\rangle = |-\rangle^{\otimes n}$ and the most excited state is $|\beta\rangle = |+\rangle^{\otimes n}$.

The coupler is pulsed periodically and the n -local coupling term varies as $\delta H = M \cos \omega t Z_1 \otimes Z_2 \dots \otimes Z_n$. From first-order time-dependent perturbation theory, we expect that there is a transition probability between the ground and the most excited state proportional to the matrix element $\langle \alpha | \delta H | \beta \rangle$. We pick the pulsing frequency $\omega = \omega_{\alpha\beta}$ to maximize the transition probability, which then grows as $M^2 t^2$ for small times. To measure this effect, we assume that we can measure state components with some n -independent constant precision ξ . To detect the state component, we must wait a time t_0 such that $M^2 t_0^2 = \xi \Rightarrow t_0 = O(1/M)$. This indicates that we require a T_2 coherence time that is at least as long and thus we need a spectral resolution of $O(M)$. This dynamic detection technique is asymptotically optimal. An illustration of this protocol is shown in Fig. 4.

For the approach to be a valid detection technique, the lower-order coupling terms cannot contribute to the

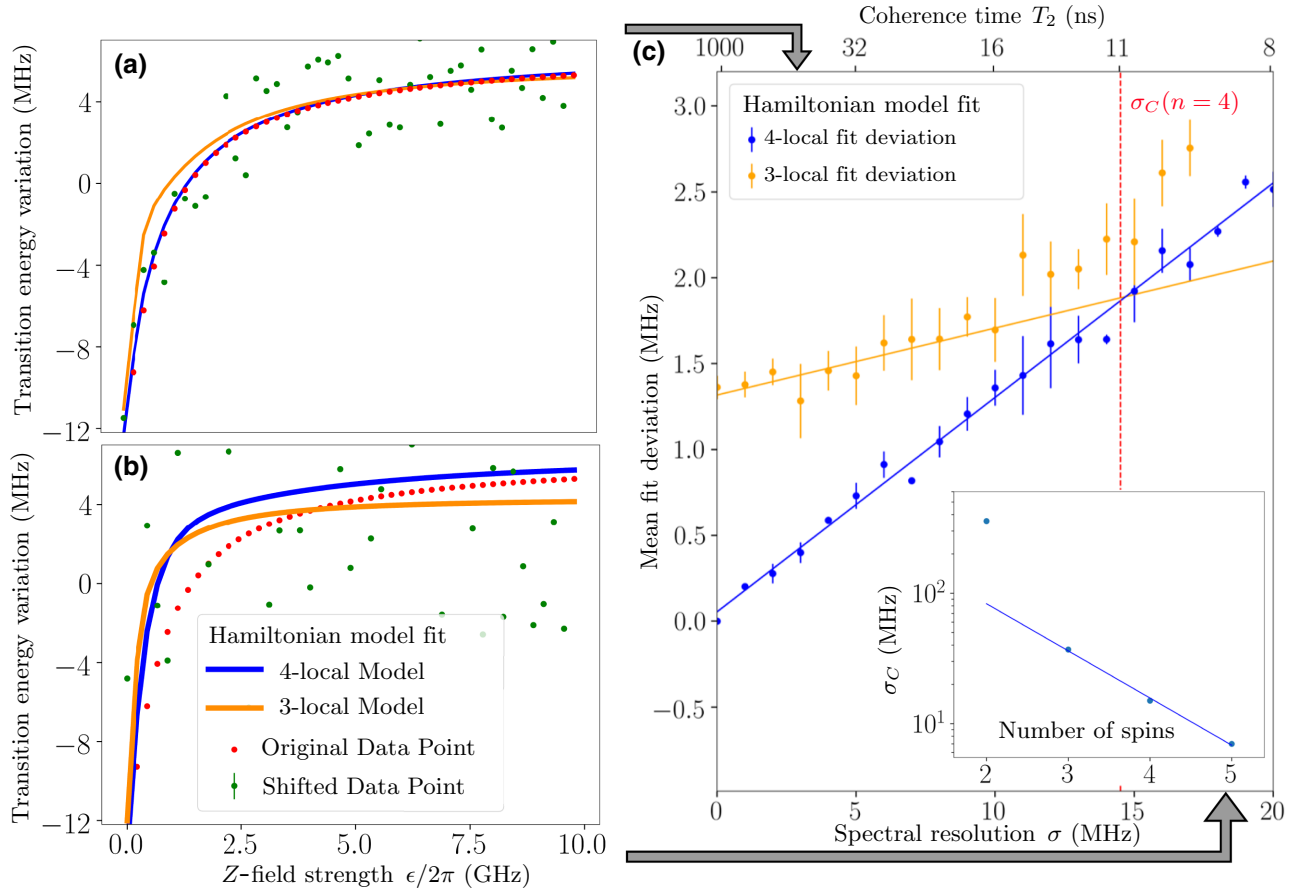


FIG. 3. The robustness of the detection method against emulated experimental error. (a) The transition-energy variation as a function of the Z field for a specific field configuration before (red dots) and after (green dots) the addition of a 5-MHz error. The 3-local (4-local) fit to the noisy data is shown in orange (blue) and the fit deviation is the mean distance between the fit and the noiseless data points. (b) The same as (a) but with an emulated error of 20 MHz. (c) A comparison of the mean fit deviation between the 3- and 4-local models as a function of the spectral resolution σ . The critical noise amplitude, which is given by the intersection point σ_C , is highlighted with the red dashed line. The inset shows the critical noise amplitude σ_C versus the number of spins n . We observe that σ_C decreases exponentially with n for a sufficiently large number of spins $n > 2$.

transition probability to first order. Using the orthogonality of the eigenstates, we find that lower-locality terms give a zero matrix element. Therefore, to first order in the strength of the n -local term M , we expect a nonzero transition probability only if the system has an n -local Hamiltonian.

The dynamic method generalizes better than the spectroscopic approach, since transition probabilities only need to be measured to a constant degree of precision, whereas the spectroscopic approach requires an exponentially decreasing spectral resolution. Another benefit is that the approach does not involve numerically expensive matrix diagonalization and fitting routines. Nevertheless, a drawback is that the coupler must be pulsed, which is a relatively strong assumption given that existing multispin coupler proposals target annealing architectures with typically limited coherence times [17–19]. Notably, the coupler must be pulsed at frequency $\omega_{\alpha\beta}$, which in this case scales with $O(n)$.

Therefore, the bandwidth of the driving source must be increased with the number of qubits or an up-conversion scheme must be implemented.

We analyze whether the method is still viable in the presence of dephasing and energy decay, using the Lindblad master equation for the system density matrix ρ :

$$\begin{aligned} \dot{\rho}(t) = & -i[H(t), \rho(t)] \\ & + \sum_i \frac{1}{2} (2C_i \rho(t) C_i^\dagger - \rho(t) C_i^\dagger C_i - C_i^\dagger C_i \rho(t)). \end{aligned} \quad (4)$$

We consider one collapse operator C_i causing the decay of single spins: $C_i = \sqrt{\gamma_i} |-\rangle_i \langle +|_i$. A second collapse operator causes dephasing: $C_i = \sqrt{\gamma_i/2} X_i$. The dephasing rate γ_i is chosen as $\gamma_i = 1/T_2$, with the energy decay and the dephasing having equal rates.

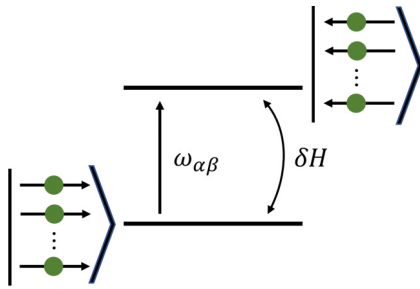


FIG. 4. An illustration of the protocol for the dynamic detection technique. The system begins in an approximate ground state of the noninteracting Hamiltonian H_0 and is excited to the most excited state under perturbation δH . This transition only exists to first order if the n -local term exists.

We analyze the method performance by analyzing the state contrast of the system during a period of 1000 ns. We define the state contrast as the difference between the maximum probability of measuring the $|+\rangle^{\otimes n}$ state minus the maximum probability of measuring any other eigenstate during the time window, excluding $|-\rangle^{\otimes n}$. If the $|+\rangle^{\otimes n}$ state is not the state with the largest probability, the state contrast is set to zero. This is a natural measure of success, as the transition to the most excited state is predominantly due to the n -local term and a sufficiently high state contrast would imply the existence of the desired term.

The time evolution of the system is simulated numerically with QuTiP [32] and the result is shown in Fig. 5. We show the state-contrast dependence on the number of spins n and the coherence time T_2 . For short coherence times, the state contrast is small, implying that a sufficiently large coherence time is required. Furthermore, the state contrast decreases as n is increased, which is expected as there are more decay pathways from the highest to lower-energy

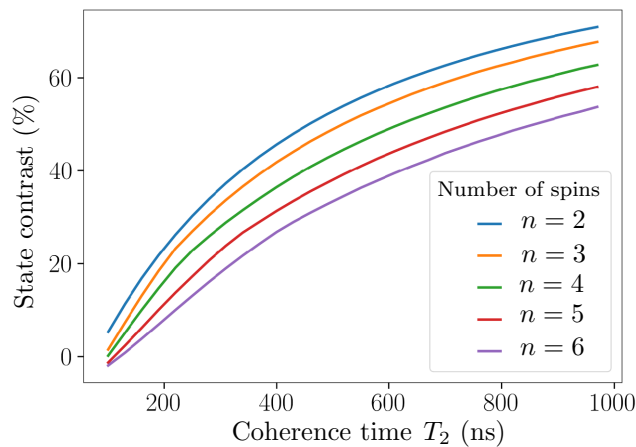


FIG. 5. A plot of the state contrast as a function of the number of spins n and the coherence time T_2 . For large enough coherence times T_2 , the state contrast is high, which implies the existence of the desired n -local term.

states. We highlight that for Hamiltonians without the n -local term, the state contrast is mostly zero—as the most excited state is rarely excited—and it never passes 10% in our simulations, thus showing that this method can prove the existence of a n -local Hamiltonian.

VII. CONCLUSIONS

We present a spectroscopic detection technique capable of characterizing n -local spin interactions. The robustness of the method against experimental errors and spurious terms is analyzed both numerically and analytically. We find that this approach is expected to perform well for systems of up to five spins. In practice, methods from quantum sensing such as Ramsey sequences could be applied to determine the transition frequency with maximum precision [33]. For larger systems, we contrast the method with an alternative technique that relies on dynamical control of the coupler and is more extensible asymptotically. While the spectroscopic method relies on sweeps of the Z fields, the dynamic method is natively applicable to fixed-frequency qubit architectures. For practical multispin coupler designs [17–19], our methods are applicable for experimentally feasible error amplitudes and thus can be used to characterize the system Hamiltonian and detect its locality.

ACKNOWLEDGMENTS

We acknowledge Thiago Bergamaschi and Jeffrey A. Grover for valuable discussions. This research was funded in part by the Office of the Director of National Intelligence (ODNI), Intelligence Advanced Research Projects Activity (IARPA) under Air Force Contract No. FA8702-15-D-0001. The views and conclusions contained herein are those of the authors and should not be interpreted as necessarily representing the official policies or endorsements, either expressed or implied, of the ODNI, IARPA, or the U.S. Government.

- [1] J. T. Seeley, M. J. Richard, and P. J. Love, The Bravyi-Kitaev transformation for quantum computation of electronic structure, *J. Chem. Phys.* **137**, 224109 (2012).
- [2] R. Babbush, P. J. Love, and A. Aspuru-Guzik, Adiabatic quantum simulation of quantum chemistry, *Sci. Rep.* **4**, 6603 (2014).
- [3] P. J. O’Malley *et al.*, Scalable Quantum Simulation of Molecular Energies, *Phys. Rev. X* **6**, 031007 (2016).
- [4] K. Majumdar, D. Furton, and G. S. Uhrig, Effects of ring exchange interaction on the Néel phase of two-dimensional, spatially anisotropic, frustrated Heisenberg quantum antiferromagnet, *Phys. Rev. B* **85**, 144420 (2012).
- [5] D. Bacon, Operator quantum error-correcting subsystems for self-correcting quantum memories, *Phys. Rev. A* **73**, 012340 (2006).

- [6] A. Kerman, Design and simulation of complex superconducting circuits for advanced quantum annealing hardware, *Bulletin of the American Physical Society* (2018).
- [7] C. Cesare, A. J. Landahl, D. Bacon, S. T. Flammia, and A. Neels, Adiabatic topological quantum computing, *Phys. Rev. A* **92**, 012336 (2015).
- [8] R. Martoňák, G. E. Santoro, and E. Tosatti, Quantum annealing of the traveling-salesman problem, *Phys. Rev. E* **70**, 057701 (2004).
- [9] G. E. Santoro and E. Tosatti, Optimization using quantum mechanics: Quantum annealing through adiabatic evolution, *J. Phys. A: Math. Gen.* **39**, R393 (2006).
- [10] M. W. Johnson *et al.*, Quantum annealing with manufactured spins, *Nature* **473**, 194 (2011).
- [11] J. Kempe, A. Kitaev, and O. Regev, The complexity of the local Hamiltonian problem, *SIAM J. Comput.* **35**, 1070 (2006).
- [12] S. P. Jordan and E. Farhi, Perturbative gadgets at arbitrary orders, *Phys. Rev. A* **77**, 062329 (2008).
- [13] M. Leib, P. Zoller, and W. Lechner, A transmon quantum annealer: Decomposing many-body Ising constraints into pair interactions, *Quantum Sci. Technol.* **1**, 015008 (2016).
- [14] N. Chancellor, S. Zohren, and P. A. Warburton, Circuit design for multi-body interactions in superconducting quantum annealing systems with applications to a scalable architecture, *Npj Quantum Inf.* **3**, 21 (2017).
- [15] A. Mezzacapo, L. Lamata, S. Filipp, and E. Solano, Many-Body Interactions with Tunable-Coupling Transmon Qubits, *Phys. Rev. Lett.* **113**, 050501 (2014).
- [16] M. Hafezi, P. Adhikari, and J. M. Taylor, Engineering three-body interaction and Pfaffian states in circuit QED systems, *Phys. Rev. B* **90**, 1 (2014).
- [17] M. Schöndorf and F. Wilhelm, Nonpairwise Interactions Induced by Virtual Transitions in Four Coupled Artificial Atoms, *Phys. Rev. Appl.* **12**, 064026 (2019).
- [18] D. Melanson, A. J. Martinez, S. Bedkihal, and A. Lupascu, Tunable three-body coupler for superconducting flux qubits, arXiv preprint [arXiv:1909.02091](https://arxiv.org/abs/1909.02091) (2019).
- [19] T. Menke, F. Häse, S. Gustavsson, A. J. Kerman, W. D. Oliver, and A. Aspuru-Guzik, Automated design of superconducting circuits and its application to 4-local couplers, *Npj Quantum Inf.* **7**, 49 (2021).
- [20] W. Liu, W. Feng, W. Ren, D.-W. Wang, and H. Wang, Synthesizing three-body interaction of spin chirality with superconducting qubits, *Appl. Phys. Lett.* **116**, 114001 (2020).
- [21] S. J. Weber, G. O. Samach, D. Hover, S. Gustavsson, D. K. Kim, A. Melville, D. Rosenberg, A. P. Sears, F. Yan, J. L. Yoder, W. D. Oliver, and A. J. Kerman, Coherent Coupled Qubits for Quantum Annealing, *Phys. Rev. Appl.* **8**, 014004 (2017).
- [22] R. Harris, A. J. Berkley, M. W. Johnson, P. Bunyk, S. Govorkov, M. C. Thom, S. Uchaikin, A. B. Wilson, J. Chung, E. Holtham, J. D. Biamonte, A. Y. Smirnov, M. H. S. Amin, and A. Maassen van den Brink, Sign- and Magnitude-Tunable Coupler for Superconducting Flux Qubits, *Phys. Rev. Lett.* **98**, 177001 (2007).
- [23] I. Ozfidan *et al.*, Demonstration of a Nonstoquastic Hamiltonian in Coupled Superconducting Flux Qubits, *Phys. Rev. Appl.* **13**, 034037 (2020).
- [24] T. Menke, W. P. Banner, T. R. Bergamaschi, A. Di Paolo, A. Vepsäläinen, S. J. Weber, R. Winik, A. Melville, B. M. Niedzielski, D. Rosenberg, K. Serniak, M. E. Schwartz, J. L. Yoder, A. Aspuru-Guzik, S. Gustavsson, J. A. Grover, C. F. Hirjibehedin, A. J. Kerman, and W. D. Oliver, Demonstration of tunable three-body interactions between superconducting qubits, (2022).
- [25] T. P. Orlando, J. E. Mooij, L. Tian, C. H. van der Wal, L. S. Levitov, S. Lloyd, and J. J. Mazo, Superconducting persistent-current qubit, *Phys. Rev. B* **60**, 15398- (1999).
- [26] J. Q. You, X. Hu, S. Ashhab, and F. Nori, Low-decoherence flux qubit, *Phys. Rev. B* **75**, 1 (2007).
- [27] F. Yan, S. Gustavsson, A. Kamal, J. Birenbaum, A. P. Sears, D. Hover, T. J. Gudmundsen, D. Rosenberg, G. Samach, S. Weber, J. L. Yoder, T. P. Orlando, J. Clarke, A. J. Kerman, and W. D. Oliver, The flux qubit revisited to enhance coherence and reproducibility, *Nat. Commun.* **7**, 1 (2016).
- [28] See the Supplemental Material at <http://link.aps.org/supplemental/10.1103/PhysRevApplied.18.044018> for an analysis of the effect of spurious terms on the static detection technique, and a perturbation theory analysis of the dynamic detection technique.
- [29] P. Krantz, M. Kjaergaard, F. Yan, T. P. Orlando, S. Gustavsson, and W. D. Oliver, A quantum engineer's guide to superconducting qubits, *Appl. Phys. Rev.* **6**, 021318 (2019).
- [30] P. Virtanen *et al.*, SciPy 1.0: Fundamental Algorithms for Scientific Computing in PYTHON, *Nat. Methods* **17**, 261 (2020).
- [31] M. Kjaergaard, M. E. Schwartz, J. Braumüller, P. Krantz, J. I.-J. Wang, S. Gustavsson, and W. D. Oliver, Superconducting qubits: Current state of play, *Annu. Rev. Condens. Matter Phys.* **11**, 369- (2020).
- [32] J. Johansson, P. Nation, and F. Nori, Qutip 2: A Python framework for the dynamics of open quantum systems, *Comput. Phys. Commun.* **184**, 1234 (2013).
- [33] C. L. Degen, F. Reinhard, and P. Cappellaro, Quantum sensing, *Rev. Mod. Phys.* **89**, 035002 (2017).